Scaling and Decoherence in the Nonequilibrium Kondo Model

Stefan Kehrein

Theoretische Physik III - Elektronische Korrelationen und Magnetismus, Universität Augsburg, 86135 Augsburg, Germany

(Received 27 October 2004; published 29 July 2005)

We study the Kondo effect in quantum dots in an out-of-equilibrium state due to an applied dc-voltage bias. Using the method of infinitesimal unitary transformations (''flow equations''), we develop a perturbative scaling picture that naturally contains both equilibrium coherence and nonequilibrium decoherence effects. This framework allows one to study the competition between Kondo effect and current-induced decoherence, and it establishes a large regime dominated by single-channel Kondo physics for asymmetrically coupled quantum dots.

DOI: 10.1103/PhysRevLett.95.056602 PACS numbers: 72.15.Qm, 72.10.Fk, 73.63.Kv

Since the first experimental observations of the Kondo effect in the Coulomb blockade regime of quantum dots [1–3], a wealth of experimental and theoretical work has addressed the properties of this highly controllable correlated electron system. If a quantum dot weakly coupled to two leads carries a net spin, resonant tunneling through the dot becomes possible and leads to a Kondoesque increase of the conductance up to the unitarity limit upon lowering the temperature [4–6]. These realizations of the Kondo effect in quantum dots have led to new questions related to the out-of-equilibrium nature of the Kondo system with a stationary current for an applied voltage bias. Despite many theoretical efforts (e.g., Refs. [7–13]), a satisfactory theory for the out-of-equilibrium Kondo effect does not yet exist. Most theoretical methods that have been developed for equilibrium [14] cannot easily be generalized to the nonequilibrium situation.

In this Letter, we focus on the case of large voltage bias $V \gg T_K$ at zero temperature ($T = 0$) as a step toward a more complete understanding of the out-of-equilibrium Kondo model. Kaminski *et al.* [10] first suggested a ''poor man's'' scaling approach, and subsequently Rosch *et al.* [11] developed a more sophisticated approach based on frequency-dependent vertices and Keldysh diagrammatics. Both groups noted that decoherence generated by the current is essential since it introduces the decoherence rate $\Gamma_{\rm rel} \propto V/\ln^2(V/T_K)$ due to nonequilibrium spin relaxation processes. However, a scaling picture in a Hamiltonian framework in which this decoherence scale emerges naturally has as yet not been developed. This Letter shows that the method of infinitesimal unitary transformations (''flow equations'') [15,16] provides such a suitable generalization of Anderson's poor man's scaling picture [17]. It allows one to study the flow of coupling constants and the ensuing phase diagram in a way that is similar to the scaling analysis of an equilibrium problem, and it establishes a large regime dominated by single-channel Kondo physics for asymmetrically coupled quantum dots.

We consider a Hamiltonian describing a spin-1/2 degree of freedom $\vec{S}$ coupled to two leads a, $a' = l, r$ with voltage bias V as an effective model for a quantum dot in the Kondo regime

$$H = \sum_{a,p,\alpha} (\epsilon_p - \mu_a) c^\dagger_{ap\alpha} c_{ap\alpha} + \sum_{a',a} J_{a'a} \sum_{p',p} \vec{S} \cdot \vec{s}_{(a'p')(ap)} \quad (1)$$

Here $\vec{s}_{(a'p')(ap)} = \frac{1}{2} \Sigma_{\alpha,\beta} c^\dagger_{a'p'\alpha} \vec{\sigma}_{\alpha\beta} c_{ap\beta}$, p, p' are momentum labels and $\mu_{l,r} = \pm V/2$. If the quantum dot can be described by an Anderson impurity model with tunneling rates $\Gamma_{l,r}$ from the left or right lead, the coupling constants are related by $J^2_{lr} = J_{ll} J_{rr}$ and $J_{ll}/J_{rr} = \Gamma_l/\Gamma_r$ (notice $J_{lr} = J_{rl}$ for hermiticity) [10].

The flow equation method [15] makes a Hamiltonian increasingly diagonal by applying a sequence of infinitesimal unitary transformations with an antihermitean generator η: $\frac{dH}{dB} = [\eta(B), H(B)]$. Here B labels a one-parameter family of unitarily equivalent Hamiltonians and has the dimension (energy)$^{-2}$: $H(B = 0)$ is the initial Hamiltonian and $H(B)$ is the unitarily equivalent Hamiltonian with matrix elements with energy differences $|\Delta E| \gtrsim B^{-1/2}$ being eliminated. This renormalization group (RG)-like separation of energy scales for $B \to \infty$ can be achieved by choosing the generator as the commutator of the diagonal and the interaction part of the Hamiltonian: $\eta(B) \times \stackrel{\rm def}{=} [H_0(B), H_{\rm int}(B)]$. In contrast to conventional scaling approaches that successively eliminate high-energy states in the Hilbert space, the flow equation method keeps all states but makes the scattering processes increasingly more energy diagonal. This method has been successfully applied to numerous equilibrium many-body problems (e.g., Refs. [18–20]), where it correctly describes the RG-flow in which the UV cutoff is identified as $\Lambda \propto B^{-1/2}$. For an out-of-equilibrium model like the Kondo model with voltage bias, the difference between state elimination and flow equation diagonalization turns out to be more fundamental (see Fig. 1); in the flow equation picture scaling below $B^{-1/2} < V$ is straightforward. In particular, the flow equation Hamiltonian $H(B)$ for $B^{-1/2} < V$ still describes the stationary current flowing across the dot since energy-diagonal scattering processes are not eliminated, which is

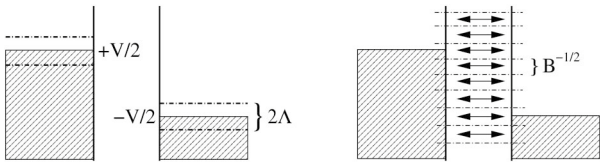

FIG. 1. Left: Conventional scaling picture where states are integrated out. Right: Flow equation approach. Here all scattering processes with energy transfer $|\Delta E| \lesssim B^{-1/2}$ are retained in $H(B)$. Both pictures depict a late phase of the flow where Λ and $B^{-1/2}$ are smaller than the voltage bias. Scattering processes between all states are taken into account in the initial phase of the flow (not depicted here).

essential for obtaining the current-induced decoherence scale.

We apply the flow equation approach with the canonical choice of η (where H_0 is the kinetic energy of the electrons) to the Kondo Hamiltonian (1). During the flow higher order interactions are generated and we parametrize the Hamiltonian as

$$H(B) = \sum_{t,\alpha} \epsilon_t c^\dagger_{t\alpha} c_{t\alpha} + \sum_{t',t} J_{t't}(B)\vec{S}\cdot\vec{s}_{t't} + i\sum_{t',t,u',u} K_{t't,u'u}(B) :\vec{S}\cdot(\vec{s}_{t't}\times\vec{s}_{u'u}):, \quad (2)$$

where $:\ldots:$ denotes normal-ordering with respect to the unperturbed Fermi sea [15]. Here t', t are general indices, initially $K_{t't,u'u}(B=0)=0$ and we neglect newly generated normal-ordered terms in $O(J^3)$ and higher. Notice that this is a nonperturbative (RG-like) approximation scheme since the coupling constant becomes a running coupling constant during the flow. Straightforward calculations lead to the following set of flow equations [21]:

$$\frac{dJ_{t't}}{dB} = -(\epsilon_{t'}-\epsilon_t)^2 J_{t't} + \frac{1}{2}\sum_u J_{t'u}J_{ut}(\epsilon_{t'}+\epsilon_t-2\epsilon_u)[n^+(u)-n^-(u)] + \frac{1}{2}\sum_{u',u} J_{u'u}(K_{u'u,t't}-K_{t't,u'u})[n^+(u')n^-(u)+n^+(u)n^-(u')](2\epsilon_u-2\epsilon_{u'}+\epsilon_t-\epsilon_{t'})+O(J^4) \quad (3)$$

$$\frac{dK_{v'v,w'w}}{dB} = -(\epsilon_{v'}+\epsilon_{w'}-\epsilon_v-\epsilon_w)^2 K_{v'v,w'w} - J_{v'v}J_{w'w}(\epsilon_{w'}-\epsilon_w)+O(J^3) \quad (4)$$

Here the Fermi sea expectation values $n^+(u) \overset{\text{def}}{=} \langle c^\dagger_u c_u\rangle$ and $n^-(u) \overset{\text{def}}{=} \langle c_u c^\dagger_u\rangle$ arise due to the normal-ordering prescription. A nontrivial test for this calculation is provided by the equilibrium case where t just describes the momentum label. Then the strong-coupling processes that determine T_K occur due to the presence of the single Fermi surface [14] and one can use the parametrization $\rho J_{p'p}(B) = g(B)\exp(-B(\epsilon_{p'}-\epsilon_p)^2)$ with the dimensionless IR-coupling constant at the Fermi level $g(B) = \rho J_{\epsilon_F\epsilon_F}(B)$. This parametrization becomes asymptotically correct in the IR limit and by inserting it in Eqs. (3) and (4), one derives the conventional third order scaling equation for the equilibrium Kondo model, $dg/d\ln\Lambda = -g^2 + g^3/2$ (with the identification $\ln\Lambda = -(1/2)\ln B$).

Equations. (3) and (4) contain complete information about the Hamiltonian flow with voltage bias to $O(J^4)$, $O(J^3)$, respectively, and can be analyzed without further approximations [21]. However, in order to gain analytical insight one can employ the following approximate parametrization that focuses on the IR limit: $\rho J_{(ap')(ap)}(B) = g_a(B)\exp[-B(\epsilon_{p'}-\epsilon_p)^2]$ with $g_a(B) = \rho J_{(a\mu_a)(a\mu_a)}(B)$ for $a = l, r$, and $\rho J_{(lp')(rp)}(B) = \rho J_{(rp)(lp')}(B) = g_t(B)\times \exp(-B(\epsilon_{p'}-\epsilon_p)^2)$ with $g_t(B) = 1/(\mu_l-\mu_r)\times \int_{\mu_r}^{\mu_l} d\epsilon \rho J_{(l\epsilon)(r\epsilon)}(B)$. Here g_l and g_r are the coupling constants for left-left and right-right scattering processes located at the respective Fermi surfaces. For g_t we choose an average over the transport couplings since this average is directly related to current and conductance [22]. Inserting these parametrizations into Eqs. (3) and (4), one arrives at the following set of equations that have to be integrated starting from $B = D^{-2}$ (D is the initial UV-band cutoff, $a = l, r$):

$$\frac{dg_a}{dB} = \frac{1}{2B}(g_a^2 + g_t^2 e^{-2BV^2}) - \frac{1}{4B^2}(k_{al}g_l + k_{ar}g_r) - \frac{1}{2B^2}k_{at}g_t(e^{-2BV^2} + V\sqrt{\pi B/2}\,\mathrm{erf}(\sqrt{2B}V)) \quad (5)$$

$$\frac{dg_t}{dB} = \frac{1}{2B}g_t(g_l+g_r)\frac{\sqrt{\pi}}{2}\frac{1}{\sqrt{2B}V}\mathrm{erf}(\sqrt{2B}V) - \frac{1}{4B^2}(k_{tl}g_l + k_{tr}g_r) - \frac{1}{2B^2}k_{tt}g_t[e^{-2BV^2} + V\sqrt{\pi B/2}\,\mathrm{erf}(\sqrt{2B}V)] \quad (6)$$

where $dk_{bc}/dB = g_b g_c$ with the initial condition $k_{bc}(B = D^{-2}) = 0$ for all $b, c = l, r, t$. The scaling picture deduced from Eqs. (5) and (6) is the main result of this Letter.

Equations (5) and (6) take different forms for $B^{-1/2} \gtrsim V$ and $B^{-1/2} \lesssim V$. We first analyze the scaling behavior down to the scale set by the voltage bias; only terms up to second order need to be taken into account here (higher order terms are unimportant for $V \gg T_K$). One arrives at a set of equations already analyzed in Ref. [10] ($a = l, r$):

$$\frac{dg_a}{dB} = \frac{1}{2B}(g_a^2+g_t^2), \qquad \frac{dg_t}{dB} = \frac{1}{2B}g_t(g_l+g_r). \quad (7)$$

In the following discussion we only look at Kondo dots described by an Anderson impurity model. The scaling invariant Kondo temperature is then set by the equilibrium case, $T_K = D\sqrt{g_l+g_r}\exp(-1/g_l+g_r)$, and one easily shows $g_t(B = V^{-2}) = (\sqrt{\Gamma_l\Gamma_r}/\Gamma_l+\Gamma_r)/\ln(V/T_K)$. From (6) one deduces that the growth of g_t effectively stops

below the voltage bias scale since there is no sharp Fermi surface for transport processes. However, looking at the second order terms in (5) the strong-coupling divergences for g_l and g_r are not cut off. This has led to the prediction of two-channel Kondo physics in Kondo dots with voltage bias [23]. But even in the weak-coupling regime third order terms in the coupling constant eventually become more important than second order terms for nonvanishing voltage bias in (5) and (6). For $B^{-1/2} \lesssim V$ the dominant terms in the flow equations are approximately (but sufficiently accurate for a qualitative picture)

$$\frac{dg_t}{dB} = -\frac{V}{\sqrt{B}}\sqrt{\frac{\pi}{8}}g_t^3 \tag{8}$$

$$\frac{dg_a}{dB} = \frac{1}{2B}\left(g_a^2 + 2g_a\frac{d\ln g_t}{d\ln B}\right) \quad \text{for } a = l, r. \tag{9}$$

The flow changes qualitatively below the *decoherence scale* $B_{\rm dec}^{-1/2} = Vg_t^2(B = V^{-2})$: for $B \gtrsim B_{\rm dec}$ algebraic decay $g_t(B) \propto B^{-1/4}$ sets in. In Eq. (9) one can then study the competition between coherent strong-coupling behavior from the second order term, and decoherence effects that arise in linear order in g_a for $B \gtrsim B_{\rm dec}$. The growth of the coupling constants g_l, g_r stops at the decoherence scale unless the coupling constants have already become too large. This qualitative analysis is confirmed by the numerical solution of the full set of Eqs. (5) and (6) depicted in Fig. 2. Also notice that current-induced decoherence enters differently from temperature into the flow Eq. (9). Temperature acts as an infrared cutoff in the Kondo strong-coupling terms $g_a^2/2B$, whereas current-induced decoherence and the coherent strong-coupling processes are *in competition*. Therefore the Hamiltonian flow derived in this Letter confirms the existence of the decoherence rate $\Gamma_{\rm rel} \propto B_{\rm dec}^{-1/2}$ due to current-induced spin relaxation [10,11]. It is essential to work in a framework where energy-diagonal processes are retained because this means that a "window" of order voltage bias is open for transport (compare Fig. 1). It is exactly these transport processes that are responsible for the emergence of the decoherence scale since they lead to the $VB^{-1/2}$ terms in (8) and (9). A conventional scaling approach that removes states around the two Fermi surfaces and therefore purports to treat energy-diagonal transport processes (see Fig. 1) cannot describe this and leads to $1/B$ terms instead [24].

Since we now know explicitly how decoherence enters into flow equations (5) and (6), we can determine a quantitative phase diagram. The scaling curves for symmetrically coupled Kondo dots in Fig. 2(a) confirm the absence of two-channel Kondo physics for large voltage bias in the sense that all couplings remain small. We define the strong-coupling regime by requiring that at least one coupling grows larger than 0.5; the resulting curve is depicted in Fig. 3 [25]. This line should not be interpreted as a phase transition; the crossover is expected to be smooth—similar to the effect of temperature in the equilibrium Kondo

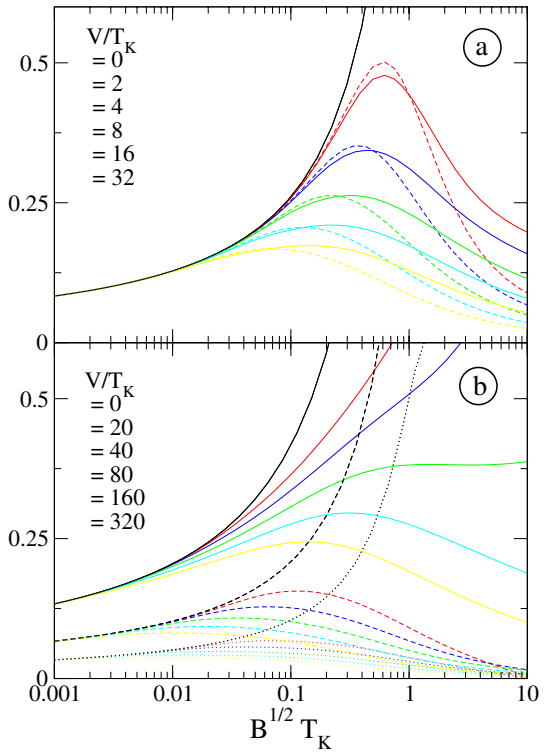

FIG. 2 (color online). Universal curves for the flow of the coupling constants g_l (solid lines), g_t (dashed lines) and g_r (dotted lines) for symmetrically coupled quantum dots [(a) with $\Gamma_l/\Gamma_r = 1$] and for an asymmetrically coupled quantum dot [(b) with $\Gamma_l/\Gamma_r = 4$]. Results are shown for various ratios $V/T_{\rm K}$ labeling the curves from top to bottom. g_l and g_r coincide in the symmetric case, therefore only g_l is shown in a.

model. For asymmetrically coupled Kondo dots this strong-coupling regime extends to remarkably large values of the voltage bias due to the "bifurcating" structure of the flow [see Fig. 2(b)] and since the decoherence scale $B_{\rm dec}^{-1/2}$ is proportional to the current I (see below); for a given ratio of $V/T_{\rm K}$ the maximum value of $I/T_{\rm K}$ is achieved for symmetrically coupled dots. Therefore current-induced decoherence is less effective in asymmetrically coupled Kondo dots when competing with the coherent interlead strong-coupling processes.

Experimentally, this phase diagram can be explored by measuring the Kondo dot density of states $\rho_d(\omega)$, e.g., via a 3-lead setup [26]. The strong-coupling regime in asymmetric Kondo dots implies a density of states at the Fermi level of the more strongly coupled lead that only drops significantly ($\lesssim$25%) below the Friedel value once $V/T_{\rm K}$ is well in the weak-coupling regime in Fig. 3. For already small asymmetries the crossover to the strong-coupling regime is driven by single-channel Kondo physics in the sense that the couplings at one Fermi surface start to dominate strongly. This effect can be traced into the weak-coupling regime by the observation that the ratio of the local density of states at the two Fermi levels is then given by $\rho_d(\mu_l)/\rho_d(\mu_r) = \alpha^2$ with $\alpha = g_l(B_l)\Gamma_r/g_r(B_r)\Gamma_l$ from Fig. 3: here B_a is defined as the B value where $g_a(B_a)$

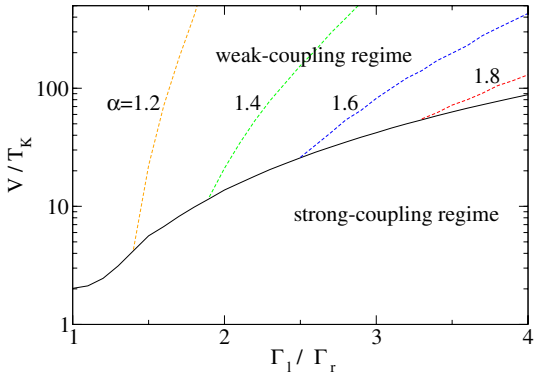

FIG. 3 (color online). Phase diagram of the nonequilibrium Kondo model as a function of asymmetry Γ_l/Γ_r and voltage bias. The solid line separates a weak-coupling regime (defined by all couplings remaining smaller than 0.5 during the entire flow) from a strong-coupling regime. The contour lines (dashed) show the ratio $\alpha = g_l(B_l)\Gamma_r/g_r(B_r)\Gamma_l$; see text.

takes its maximum value and the expression for α follows from a conventional Keldysh calculation [11] with the effective Hamiltonian $H(B)$ on this scale [27]. The observation $\rho_d(\mu_l)/\rho_d(\mu_r) \neq 1$ in asymmetric Kondo dots has also been made in other approaches though without obtaining a quantitative phase diagram (compare Refs. [11,26,28]).

A final remark regarding the calculation of observables: these need to be unitarily transformed as well [18] (they typically change their form completely once $B \gtrsim B_{\rm dec}$). For example, the current operator remains form invariant with the flowing coupling $g_t(B)$ up to scale $B_{\rm dec}$: $I(B) = ig_t(B)\sum_{p',p} \vec{S}\cdot(\vec{s}_{(lp')(rp)} - \vec{s}_{(rp')(lp)})$. One can then work with the renormalized effective Hamiltonian on the scale $B_{\rm dec}$ and a conventional Keldysh calculation yields $I = (3\pi/4)Vg_t^2(B_{\rm dec})$. This leads to the well-known perturbative result for the conductance [10] $G(V) = G_{\rm u}(3\pi^2/16)/\ln^2(V/T_{\rm K})$ where $G_{\rm u} = (e^2/\pi\hbar)4\Gamma_l\Gamma_r/(\Gamma_l+\Gamma_r)^2$ is the conductance in the unitarity limit. Notice that transport quantities are not low-energy properties like the Kondo dot density of states at the Fermi levels and are therefore unaffected by the strong-coupling physics in Fig. 3 as long as $V \gg T_{\rm K}$.

Summing up, we have developed a Hamiltonian scaling picture for Kondo dots with voltage bias that allows us to express physical quantities in terms of renormalized parameters. We confirm the absence of two-channel Kondo physics for symmetrically coupled quantum dots, and show the existence of a large regime dominated by single-channel strong-coupling physics for asymmetric dots.

I thank J. von Delft, D. Vollhardt, and F. Wegner for valuable discussions, and acknowledge valuable discussions about this and related subjects with N. Andrei and B. Doyon. This work was supported in part by SFB 484 of the Deutsche Forschungsgemeinschaft (DFG) and by the Heisenberg program of the DFG.

[1] D. Goldhaber-Gordon *et al.*, Nature (London) **391**, 156 (1998).
[2] S. M. Cronenwett, T. H. Oosterkamp, and L. P. Kouwenhoven, Science **281**, 540 (1998).
[3] J. Schmid, J. Weis, K. Eberl, and K. von Klitzing, Physica (Amsterdam) **258B**, 182 (1998).
[4] L. Glazman and M. Raikh, JETP Lett. **47**, 452 (1988).
[5] T. K. Ng and P. A. Lee, Phys. Rev. Lett. **61**, 1768 (1988).
[6] W. G. van der Wiel *et al.*, Science **289**, 2105 (2000).
[7] J. Appelbaum, J. C. Phillips, and G. Tzouras, Phys. Rev. **160**, 554 (1967).
[8] J. Sólyom and A. Zawadowski, Phys. Kondens. Mater. **7**, 325 (1968); **7**, 342 (1968).
[9] J. König, J. Schmid, H. Schoeller, and G. Schön, Phys. Rev. B **54**, 16820 (1996).
[10] A. Kaminski, Yu. V. Nazarov, and L. I. Glazman, Phys. Rev. Lett. **83**, 384 (1999); Phys. Rev. B **62**, 8154 (2000).
[11] A. Rosch, J. Paaske, J. Kroha, and P. Wölfle, Phys. Rev. Lett. **90**, 076804 (2003); J. Paaske, A. Rosch, and P. Wölfle, Phys. Rev. B **69**, 155330 (2004); J. Paaske, A. Rosch, J. Kroha, and P. Wölfle, Phys. Rev. B **70**, 155301 (2004).
[12] A. Schiller and S. Hershfield, Phys. Rev. B **51**, R12896 (1995); **58**, 14978 (1998).
[13] O. Parcollet and C. Hooley, Phys. Rev. B **66**, 085315 (2002).
[14] For an overview see, e.g., A. C. Hewson, *The Kondo Problem to Heavy Fermions* (Cambridge Univ. Press, Cambridge, England, 1993).
[15] F. Wegner, Ann. Phys. (Leipzig) **3**, 77 (1994).
[16] See also S. D. Głazek and K. G. Wilson, Phys. Rev. D **48**, 5863 (1993); **49**, 4214 (1994).
[17] P. W. Anderson, J. Phys. C **3**, 2436 (1970).
[18] S. Kehrein and A. Mielke, Ann. Phys. (Leipzig) **6**, 90 (1997).
[19] I. Grote, E. Körding, and F. Wegner, J. Low Temp. Phys. **126**, 1385 (2002); V. Hankevych, I. Grote, and F. Wegner, Phys. Rev. B **66**, 094516 (2002).
[20] S. Kehrein, Phys. Rev. Lett. **83**, 4914 (1999); Nucl. Phys. **B[FS592]**, 512 (2001); W. Hofstetter and S. Kehrein, Phys. Rev. B **63**, 140402(R) (2001).
[21] Details of this calculation will be published separately.
[22] This approximation is not always accurate, e.g., for describing the flow of $J_{(l\mu_r)(l\mu_r)}$ or $J_{(l\mu_r)(r\mu_r)}$ for $B^{-1/2} \lesssim V$. However, parametrizations with more coupling constants do not modify our conclusions and we work with the minimum number necessary.
[23] P. Coleman, C. Hooley, and O. Parcollet, Phys. Rev. Lett. **86**, 4088 (2001).
[24] One can also verify that higher order terms beyond the order taken into account in (5) and (6) are smaller than the terms calculated here as long as all the coupling constants remain sufficiently small during the entire flow.
[25] This crossover line only depends weakly on the specific value for the running coupling constant that determines the strong-coupling regime (here 0.5); it is, e.g., hardly changed for a value of 1.0. Higher orders in the calculation can also shift this line, though the third order results shown here are expected to be a reliable approximation.
[26] E. Lebanon and A. Schiller, Phys. Rev. B **65**, 035308 (2002).
[27] Close to the crossover line the number α^2 is a lower bound for the asymmetry: the real ratio will be larger [21].
[28] M. Krawiec and K. I. Wysokinski, Phys. Rev. B **66**, 165408 (2002).